Cold Regions Science and Technology 120 (2015) 168–178

Contents lists available at ScienceDirect

Cold Regions Science and Technology

journal homepage: www.elsevier.com/locate/coldregions

Relating simple drivers to snow instability

Benjamin Reuter *, Alec van Herwijnen, Jochen Veitinger, Jürg Schweizer

WSL Institute for Snow and Avalanche Research SLF, Davos, Switzerland

ARTICLE INFO

Article history:
Received 30 December 2014
Received in revised form 6 May 2015
Accepted 29 June 2015
Available online 4 July 2015

Keywords:
Snow stability
Spatial variability
Terrain
Avalanche forecasting

ABSTRACT

Snow layers form during and after accumulation due to the interaction of meteorological and physical processes. It is known that the vertical structure and also the lateral continuity of layers depend on these processes and the boundaries set by the terrain. This study addresses the variations seen among vertical penetration resistance profiles and investigates possible forcings at the basin scale. In the past years we acquired a unique dataset with 613 snow micro-penetrometer (SMP) resistance measurements covering a variety of dry-snow conditions. With recent advances in signal processing all snow layer properties required for snow instability modeling are extracted from a SMP signal so that quantitative metrics of the propensity to failure initiation and crack propagation can be calculated. The modeled values of instability corresponded well with field test results obtained during the measurement campaigns and the verified, local danger. We then analyzed whether snow instability was related to simple drivers such as slope aspect, snow depth, and slope angle. In general, aspect was the most prominent driver as on all field days we found associations of our measures of snow instability with aspect. For 'old' slab layers the relation between aspect and snow instability was more pronounced than for recently deposited slab layers. However, the relationships between drivers and our measures of snow instability varied depending on whether we analyzed the single field days separately or jointly. Considering all field days jointly, which reflects mean trends over varying snowpack conditions, slope angle was weakly related to the failure initiation propensity and snow depth to the crack propagation propensity. Our findings suggest that with SMP field measurements differences in snow conditions can be resolved which relate to the failure initiation and crack propagation propensity relevant for snow instability assessment. Our analysis of terrain and snow depth data showed that readily and widely available simple drivers have the potential to enhance snow instability predictions from point measurements at the basin scale.

1. Introduction

Classical snow instability observations require an in-depth knowledge on site selection (e.g., Landry et al., 2004; Schweizer and Jamieson, 2010), snow profiling technique and above all interpretation (e.g., Schweizer and Jamieson, 2007). As we often already know the general avalanche conditions within a region, but are interested in local differences, we may look at the drivers responsible for snow instability patterns. The causes (or drivers) of spatial variations in snow instability, and in general of snowpack properties, can be divided into external and internal agents acting during and/or after deposition (Sturm and Benson, 2004). These process drivers include precipitation, wind, radiation, temperature and snow metamorphism; they all cause spatial variations mainly by interacting with terrain (Schweizer et al., 2008b). Whereas at the slope scale, the causes of spatial variations are difficult to explain since typical drivers such as radiation do hardly vary, the problem is perceived to be somewhat less complex at the basin scale (for a definition of scales used in spatial variability studies see Schweizer and Kronholm, 2007). In fact, at the scale of a basin, covering several slopes within a subregion of a valley, it has been shown that, for example, differences in snow depth can be explained to a large extent by the average wind speed, altered by terrain (Schirmer et al., 2011). Just by applying a simple terrain parameter based model (Winstral et al., 2002) they were able to reproduce general snow accumulation patterns at the basin scale. Therefore, we hypothesize that at the basin scale variations of snowpack properties relating to instability may be mainly due to varying topography so that simple drivers such as terrain parameters can be considered instead of the process drivers to explain observed spatial patterns. In contrast, this assumption does not hold at the slope scale, where these variations of topography simply do not exist.

Exploiting simple drivers such as terrain parameters or snow depth for snow instability estimation may be useful when making decisions in the field or interpolating snow instability information. Snow instability assessment is basically based on weighing meteorological conditions such as new snow accumulation, snow temperature and wind with snowpack stratigraphy and terrain (Schweizer et al., 2003a). Accounting for detailed terrain characteristics is key for accurately modeling

* Corresponding author. Tel.: +41 81 417 0347; fax: +41 81 417 0110.
E-mail address: reuter@slf.ch (B. Reuter).

http://dx.doi.org/10.1016/j.coldregions.2015.06.016

incoming global radiation (Helbig et al., 2010) and thus snow temperatures, but also for assessing snow accumulation which is forced by local, terrain induced winds (Dadic et al., 2010). As both, the radiation balance and snow accumulation are closely tied to terrain parameters, the terrain parameters aspect and slope angle are believed to shape snow instability patterns (Schweizer et al., 2008b). Moreover, slope angle is not only an important parameter of incoming short wave radiation, but also directly determines the stress state within the snowpack. Snow depth is suspected to be an indicator of snow instability, just as recurring snow depth patterns are shaped by terrain and average weather conditions (Grünewald et al., 2010). Above all, simple drivers have the great advantage that they are readily and widely available.

Various studies have investigated associations between snow instability and simple drivers such as slope aspect, snow depth and slope angle. At the slope scale, Campbell and Jamieson (2007) performed Rutschblock (RB) tests on rather uniform slopes with small differences in either aspect, snow depth or slope angle. Their results were mostly inconclusive, as on most slopes they could not find a clear relation between RB score and snow depth, aspect or slope angle. Furthermore, when correlations were present, e.g. for snow depth and slope angle, they were either positive or negative. Birkeland et al. (1995) measured snow strength with a digital resistograph as an indicator of snow instability on two different slopes. Whereas they found no relation between snow depth and snow strength at one site, they suspected less complex terrain characteristics at a second site to cause a significant relation between snow depth and snow strength.

At the regional scale, however, some studies identified relations between snow stability test results or specific snow instability related properties and terrain parameters. Birkeland (2001) was among the first to investigate the dependence of snow instability on terrain and found lower stability results in high elevation north-facing slopes. His results also indicate that differences evolve with time, i.e. variable weather conditions shape the snowpack and introduce terrain driven differences. Schweizer et al. (2003b) analyzed snow instability observations from five periods during a winter season covering a mountain region as well. Among the simple drivers specified above they found that snow depth was the best indicator of snow instability. Assessing the predictive power of meteorological and snowpack properties for observed snow instability, Zeidler and Jamieson (2004) also found snow depth to be a significant driver for instability, which they described with a skier stability index.

At the basin scale, Schweizer et al. (2008a) performed manual observations of snow surface properties and measurements of penetration resistance with the snow micro-penetrometer (SMP) (Schneebeli and Johnson, 1998). With the penetration resistance measurements (four per manual observation) they found a larger amount of variation in snow surface properties than with manual observations indicating that variation depends on measurement support, the area represented by each sample. They also explored the causes of the snow surface hardness variations based on measurements of a nearby automatic weather station. Whereas their analysis of the causes of variability at the slope scale was mainly inconclusive, they observed a general trend to lower penetration resistance in the topmost 2 cm and lower slope-scale variation after a snowfall event and higher resistance and variability during a subsequent period of fair weather.

Buried surface hoear layers can cause widespread avalanching and periods of poor snow stability. Hence, a couple of studies focused on how terrain parameters drive the distribution of surface hoar. Lutz and Birkeland (2011) modeled the radiation budget in forest openings including the sky visibility and found that spatial differences of measured surface hoar size depended thereof. Feick et al. (2007) and Borish et al. (2012) identified a correlation between elevation and surface hoar crystal size and snow instability estimates, which both attributed to local wind regimes. Schweizer and Kronholm (2007), on the other hand, found aspect and slope angle to be more indicative for the presence of surface hoar at the regional scale. Slope angle and aspect were also rated as important drivers of surface hoar formation and persistence by Helbig and van Herwijnen (2012) who modeled surface hoar size in complex terrain based on simple terrain characteristics. Horton et al. (2015) observed surface hoar sizes at a regional scale; they suggested air humidity, wind speed and surface temperature to be responsible for surface hoar formation along elevation bands. Their model results obtained from snow cover modeling coupled to numerical weather prediction output, however, were less conclusive.

In summary, the above mentioned spatial variability studies investigated if simple terrain characteristics or snow depth were associated with either snow instability observations or weak layer properties. In particular cases, such as the formation of surface hoar, drivers were identified. With regard to snow instability, however, weak layer and slab layer properties interact together which complicates the influences of drivers. Currently, it is not clear whether and when differences in snow instability can be explained by simple drivers.

Snow depth distributions in catchments or basins have successfully been modeled, but with a focus on estimating snow water equivalent or ablation rather than on snow instability prediction. Winstral et al. (2009) obtained realistic snow depth distributions from terrain, vegetation and wind data in catchments of 0.26 km^2 to 14 km^2 by including the upwind topography and employing a sheltering index. Mott and Lehning (2010) even included micro-meteorological processes such as preferential deposition and true redistribution and were able to model small-scale deposition patterns, such as dunes and cornices. Terrestrial laser scanning (TLS) is widely used to measure the spatial distribution of snow depositions (Prokop, 2008) and study ablation rates (Grünewald et al., 2010). Modeled snow distributions have been validated with this technique and exhibited recurring patterns with elevation, slope and aspect being the most important predictors (Grünewald et al., 2013). Grünewald et al. (2010) compared terrestrial and airborne laser scans from the same area and found a deviation of around 10 cm depending on the incident angle of the beam and footprint size. Using LIDAR methods spatial distributions of snow depth can be measured with high spatial resolution. A link between spatial distributions of snow depth and snow instability that could support snow instability mapping in data sparse areas, however, is pending. Also, a detailed comparison between snow instability and terrain parameters seems interesting since digital elevation models are widely available and may enhance spatial snow instability mapping. Both ideas, however, require a method for closely spaced snow instability measurements or spatially distributed snow instability modeling for comparison with LIDAR snow depth measurements or terrain parameters from digital elevation models.

The snow micro-penetrometer offers an objective way to measure snow mechanical properties relevant for slab avalanche release at high spatial resolution (Reuter et al., 2013) and to derive measures of instability (Schweizer and Reuter, 2015). In particular, a recently developed approach to determine the propensity of failure initiation and crack propagation now allows evaluating field measurements of snow stratigraphy in view of snow instability (Reuter et al., 2015). With this approach we are now able to obtain observer independent metrics of snow instability in a rapid way allowing spatial sampling with more than 100 measurements per day—exceeding former frequencies of manual stability observations.

To investigate whether snow instability is tied to simple drivers, we present snowpack and terrain data from five situations in a small basin. For every situation snow instability was derived from more than 100 SMP profiles with the approach described by Reuter et al. (2015) which allows assessing the influence of potential drivers on the propensity of failure initiation and crack propagation separately. The drivers include slope aspect, snow depth and slope angle. Driver data were available at high-resolution for the entire basin from an elevation model with 1 m horizontal resolution and repeated laser scans of the snow surface resulting in snow surface elevation models with the same resolution. Results showed associations between simple drivers and snow instability with potential to support snow instability mapping in data sparse areas.

2. Methods

In the following we describe our field data set, the processing of SMP signals including the derivation of snow instability, the derivation of terrain and snow depth data and the multiple regression analysis of simple drivers.

2.1. Field data

In the winter seasons between 2010 and 2013 we carried out five field campaigns at the Steintälli field site above Davos (Switzerland) under different snow conditions. The field site is located in a bowl draining to the east above a small ski area. The entire sampling area spans about 400 m × 400 m and was divided into 25 cells (Fig. 1) each of which has six measurement locations. Hence, considering the framework for spatial variability studies introduced by Blöschl and Sivapalan (1995), our sampling design has an extent (the longest distance between two measurement locations, or the area covered by the study) of several hundred meters, a variable spacing (the distance between measurement locations) ranging from 3 to about 80 m, and a support (the area or volume over which each measurement is integrated) of about 1 cm^2.

We recorded snow depth, slope angle and aspect of the snow surface at every SMP measurement location. Also, GPS coordinates were recorded at the corner points shown in Fig. 1. Nine manual snow profiles were concurrently observed including snow grain type and size, and hand hardness index. The profiles were complemented with stability tests and provide a valuable benchmark for snow instability. Stability tests included the propagation saw test (Gauthier and Jamieson, 2008b), the extended column test (Simenhois and Birkeland, 2009) and the compression test (Jamieson and Johnston, 1997). On each day, we also verified the avalanche danger forecast based on common field observations such as signs of instability (e.g., Haladuick et al., 2014; Jamieson et al., 2009); the verified danger level is described according to the European avalanche danger scale: low (1), moderate (2), considerable (3), high (4) and very high (5).

2.2. SMP signal analysis

In order to derive snow mechanical properties from SMP penetration resistance profiles, the signal was processed to obtain the characteristic set of microstructural parameters, namely rupture force (f), deflection at rupture (δ) and structural element size (L) (Löwe and van Herwijnen, 2012). This step involved 2.5 mm moving window averaging with an overlap of 50% and eventually yields a resolution of 1.25 mm. For the sake of shorter computation times we reduced the resolution again and introduced layers. By comparing the SMP signal to the manual snow profiles, with a particular focus on the most critical weakness found in stability tests, every SMP signal was divided into several slab layers, a weak layer and a basal layer. For those layers the average mechanical properties were calculated as follows. Snow density ρ was derived after Proksch et al. (2014) who refined previous penetration resistance based approaches by including the structural element length L:

$$\rho = a_1 + a_2 \log\left(\tilde{F}\right) + a_3 L \log\left(\tilde{F}\right) + a_4 L \tag{1}$$

where a_i are coefficients, F is the penetration resistance and tilde denotes the median. The weak layer fracture energy w_f was derived after Reuter et al. (2013) who showed that integrating the penetration resistance over a window of 2.5 mm and taking the minimum across the weak layer yielded plausible values compared with particle tracking velocimetry results of propagation saw tests (van Herwijnen and Heierli, 2010). From the micro-structural parameters, deflection at rupture δ, structural element size L and rupture force f, the effective modulus E and the strength σ were calculated after Johnson and Schneebeli (1999):

$$E = \frac{f}{\delta L} \tag{2}$$

$$\sigma = \frac{f}{L^2}. \tag{3}$$

Thus, at every SMP measurement location, snow stratigraphy was characterized by the relevant mechanical properties: ρ and E for the slab layers, w_f and σ_{WL} for the weak layer, and ρ and E for the basal layers. Following the recently presented approach by Reuter et al. (2015) the failure initiation criterion and the critical crack length were derived as estimates of snow instability.

2.3. Failure initiation criterion

As described by Reuter et al. (2015), a criterion S describing the likelihood of initiating a failure at the depth of the weak layer was defined as:

$$S = \frac{\sigma_{WL}}{\Delta\tau}, \tag{4}$$

with σ_{WL} the strength of the weak layer and $\Delta\tau$ the maximum shear stress within the weak layer due to skier loading only. The maximum shear stress under the stratified slab was modeled by a finite element simulation (Habermann et al., 2008). As SMP derived values of strength are larger by about two orders of magnitude than values of shear strength found in literature (Marshall and Johnson, 2009), the values of S are much higher than typical values of e.g. the skier stability index (Jamieson and Johnston, 1998). Nonetheless, Reuter et al. (2015) showed that S was clearly related to Rutschblock scores.

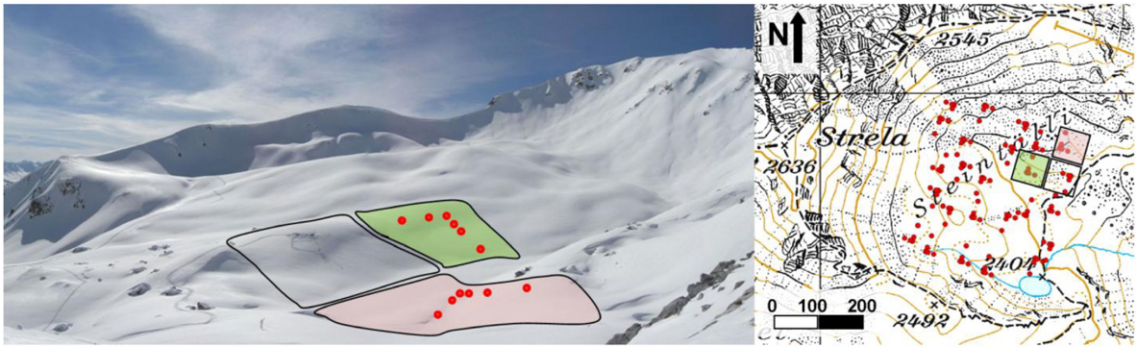

Fig. 1. On the left, photography of the Steintälli field site (looking towards the southwest) with 3 out of 25 cells, one with field staff at work (No. 16) and two (No. 17 and No. 21) with sampling locations (red dots). On the right, map showing the field site with sampling locations (contour line interval is 20 m). Red dots indicating SMP profiles and measurements of terrain parameters and snow depth.

2.4. Crack propagation propensity

The snowpack's propensity to support crack propagation in a weak layer may be estimated as the critical crack length r_c for unstable crack propagation. The critical crack length was obtained by finding the real, positive root of the formulation of the specific fracture energy w_f given by Eq. (4) in Schweizer et al. (2011):

$$w_f(E, r_c) = \frac{H}{2E}\left[w_0 + w_1\frac{r_c}{H} + w_2\left(\frac{r_c}{H}\right)^2 + w_3\left(\frac{r_c}{H}\right)^3 + w_4\left(\frac{r_c}{H}\right)^4\right], \quad (5)$$

with

$$w_0 = \frac{3\eta^2}{4}\tau^2,$$

$$w_1 = \left(\pi\gamma + \frac{3\eta}{2}\right)\tau^2 + 3\eta^2\tau\sigma + \pi\gamma\sigma^2,$$

$$w_2 = \tau^2 + \frac{9\eta}{2}\tau\sigma + 3\eta^2\sigma^2,$$

$$w_3 = 3\eta\sigma^2,$$

$$w_4 = 3\sigma^2,$$

with E as the elastic modulus, H as the slab thickness, $\eta = \sqrt{4(1+\nu)/5}$, $\gamma = 1$ as the mismatch parameter, ν as the Poisson's ratio, $\tau = -\rho g H \sin(\alpha)$ $H\sin(\alpha)$ as the shear stress and $\sigma = -\rho g H \cos(\alpha)$ as the normal stress including density ρ, gravity g and slope angle α. This approach requires an assumption about the elastic modulus E of the entire slab, i.e. the bulk modulus. Following Reuter et al. (2015) we used the bulk effective modulus obtained from finite element simulations to account for snow stratigraphy, as assuming a uniform slab results in inaccurate estimates of the mechanical deformation energy (Schweizer et al., 2011).

2.5. Drivers

Our list of drivers is confined to easily available parameters and hence only includes slope aspect, snow depth and slope angle. The influence of each of these drivers may be on snowpack properties directly and/or indirectly by affecting the meteorological processes and thereby shaping snowpack properties.

2.5.1. Slope aspect and slope angle

Slope aspect and slope angle of the snow surface were available from manual observations at every SMP measurement location, but also from a 1 m-resolution digital elevation model (DEM) covering the Steintälli field site. The digital elevation model data were used to compare the terrain properties at the sampling locations with the distribution characteristic of the basin.

Slope aspects are not equally represented in our field site according to calculations from digital elevation model data (Fig. 2a). Our samples show the same uneven distribution with considerably more members between north–east and south than between south–west and north in a clockwise sense. We consider our samples representative of the field site, as distributions have similar characteristics, sampling locations were selected randomly in the 25 grid cells and the observation density is about one per 1000 m^2 on average.

Rather than splitting the compass rose into four or eight sections and introducing classes, we introduced continuous weighting functions for aspects. We used the first two terms of a Fourier series expansion (Fig. 3) to characterize the observed aspects. The aspect variable asp_{E-W} gives aspects with an easterly component a higher weight ($asp_{E-W} = 1$) than those with a westerly component ($asp_{E-W} = -1$). We consider this variable as our field site lies in a small basin which opens to the east and is sheltered to the west. The aspect variable asp_{N-S} weighs northerly ($asp_{N-S} = 1$) against southerly aspects ($asp_{N-S} = -1$). This transformation basically models the course of the sun. For example, for the aspect SE (=135°) the values of the aspect variables are asp_{E-W} (135°) = 0.71 and asp_{N-S} (135°) = −0.71, whereas for E (=90°) they are 1 and 0, respectively.

Our samples of slope angles were almost normally distributed with a maximum ($N = 187$) in the range of 15-20° (Fig. 2b). From digital elevation model data of the entire field site we know that the distribution of slope angles also peaks between 15° and 20° indicating that our samples are representative of the field site characteristics.

2.5.2. Snow depth and slab depth

The distribution of snow depth in our data set was almost normally distributed with a mean of 1.65 m and was slightly skewed to lower values (median 1.52 m). Also for the snow depth, our samples can be considered as representative of the field site's snow depth distribution as laser scan derived snow depths of the same day had very similar almost Gaussian distributions (Fig. 2c). We explore snow depth data from manual measurements close to SMP measurement locations and repeated laser scans of the Steintälli field site. Snow distribution in the Steintälli basin was determined by terrestrial laser scanning (TLS) using the Riegl LPM-321 device operating at 905 nm (Veitinger et al., 2014). Prokop (2008) and Prokop et al. (2008) demonstrated the suitability of this scanner for snow depth measurements in alpine terrain. Grünewald et al. (2010), by comparing TLS with Tachymeter measurements, established a mean deviation of 4 cm with a standard deviation of 5 cm at distances up to 250 m. In order to georeference the scans, we installed six reflector plates at different distances and angles from the scanner position. The plates were attached to existing weather stations or drilled into rockwalls; this assured stable positions over the 3-year measurement period. The laser scanner was mounted

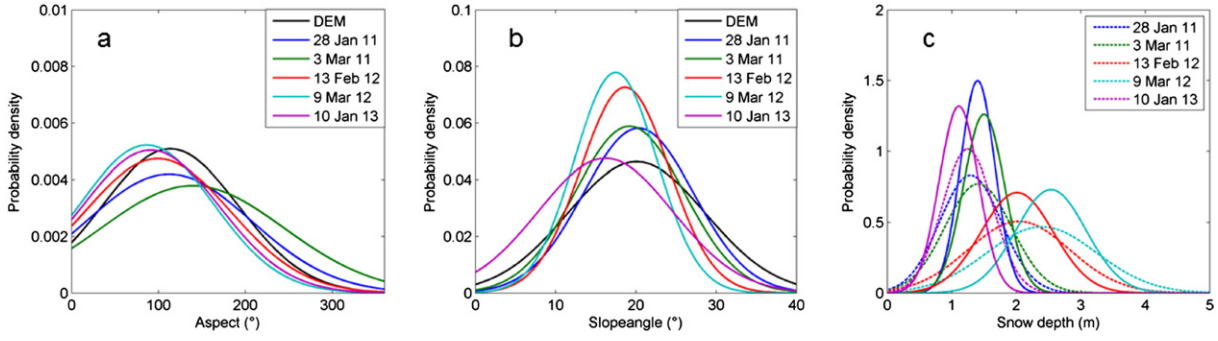

Fig. 2. Probability density functions fitted to terrain parameters normalized by area. (a) For aspects derived from DEM (black line) and from manual field measurements on the indicated dates (colored lines). (b) For slope angles derived from DEM (black line) and from manual field measurements on the indicated dates (colored lines). (c) For snow depth on the indicated dates derived from TLS (colored dashed lines) and from manual field measurements (colored solid lines).

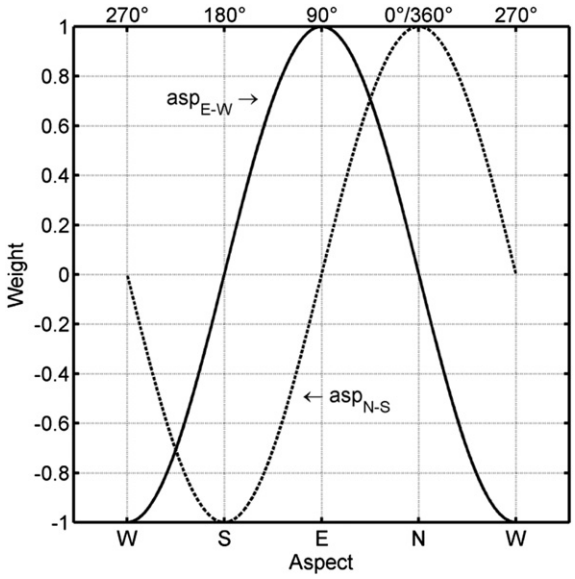

Fig. 3. Aspect weighting variables asp_{E-W} (full line) and asp_{N-S} (dotted line) as derived from the two first terms of a Fourier series expansion. The variable asp_{E-W} weighs easterly ($asp_{E-W} = 1$) with westerly aspects ($asp_{E-W} = -1$) and asp_{N-S} weighs northerly ($asp_{N-S} = 1$) with southerly aspects ($asp_{N-S} = -1$).

on a tripod on a small hill overlooking the Steintälli basin. The tripod was installed on solid rock to minimize vibration effects due to wind and keep errors due to settling and tilting small. In order to obtain snow depth, elevations measured with the laser scanner were subtracted from a digital terrain model created with the same technique. As scan data were available at very high resolution, the presented maps have a horizontal resolution of 1 m. Some areas of the field site cannot be seen from this location and hence the TLS data do not cover the entire area. Data gaps were filled by nearest neighbor interpolation.

In addition to snow depth we also considered slab depth. Slab depth which is equivalent to the depth of the weak layer was derived from SMP measurements. Slab depth affects failure initiation as well as crack propagation propensity (van Herwijnen and Jamieson, 2007) so that spatial variations of instability may well be related to slab depth. However, slab depth cannot be considered as readily available variable, and we therefore did not include it in the multiple linear regression analysis (see below), but only performed a simple correlation analysis.

2.5.3. Representativity of field samples

In order to assess if the samples we collected in the field were representative of the basin we compared our field sample distributions of aspect, slope angle and snow depth with the distribution of the terrain parameters from the DEM and of snow depth from TLS. Therefore, we resampled the DEM as well as the TLS data 100 times each in the sampling area to obtain comparable sample sizes and performed a *U*-test (Table 1). In 9 out of 15 cases the majority of the repeated tests indicated that our field samples were representative of the entire basin. On 3 March 2011 and 13 February 2012 samples were representative for all parameters, whereas this was not always the case on the other field days. Still, comparing the distributions visually (Fig. 2) suggests that distribution were rather similar.

2.6. Relating snow instability to simple drivers

In order to assess the predictive power of simple drivers for point snow instability, we used a stepwise method of multiple linear regressions (MLR) (Draper and Smith, 1998). The presumed drivers slope angle, aspect and snow depth were fed into MLR models as predictors. The dependent variable was either the modeled failure initiation criterion S or the modeled critical crack length r_c. For this analysis a regression model was created by stepwise increasing the number of predictors until the predictive power did no longer improve significantly resulting in a final model (F-test, significance level $p = 0.05$). We report the p-values for testing if a coefficient is not zero. Only drivers with p-values $p \le 0.05$ appear in the final model and the reported p-values refer to the final model. For excluded predictors the p-value is reported that would result if the predictor was included in the final model. We consider drivers as relevant if their regression coefficient standard error $\Delta(r) < 50\%$ and their p-value $p \le 0.05$.

Moreover, the Pearson correlation coefficient r_p, the Spearman rank order correlation coefficient r_s and the value of significance p of the regression slope assuming significance for $p < 0.05$ are presented to describe the strength of linear relations.

3. Results

3.1. General avalanche conditions

Three out of five field campaigns we carried out on days with 'moderate' avalanche danger. In one case the avalanche danger was rated 'low' and in another case 'considerable' (Table 2). In Fig. 4 we present maps of snow depth anomaly from the daily mean with modeled point snow instability estimates for 3 March 2011 and 13 February 2012. On these days the danger level was 'considerable' and 'moderate', respectively, which is reflected in both instability criteria: on 3 March 2011 the average modeled critical crack length ($r_c = 26$ cm) was lower than on 13 February 2012 ($r_c = 48$ cm). Also the average of the failure initiation criterion yielded lower values on 3 March 2011 ($S = 167$) than on 13 February 2012 ($S = 238$).

Overall, the modeled critical crack length was lowest for days with 'considerable' avalanche danger with a median of $r_c = 0.26$ m (Fig. 5). In those cases when the avalanche danger was rated 'moderate' the median critical crack length was $r_c = 0.42$ m. Interestingly, modeled values of r_c were lower on 28 January 2011 (median $r_c = 0.36$ m), when the avalanche danger was rated 'low'. Also, the results of the crack propagation tests rather indicated that cracks may propagate: PST 46/120 cm END on an east-facing slope, ECT 11/11 on a south-facing slope and ECT 23/pp on a north-facing slope. But due to the soft slab, widespread crack propagation was deemed unlikely. We measured an average penetration force of 0.07 N and a density of 112 kg m^{-3} of the surface slab layer with the SMP. About 1 month later, on 3 March 2011, the same weak layer was buried deeper and the danger level

Table 1
Percentage of representative cases of field samples according to the *U*-test for terrain parameters and snow depth by field days.

Date	Slope angle	Aspect	Snow depth
28 January 2011	97	85	33
3 March 2011	95	87	76
13 February 2012	77	65	96
9 March 2012	29	9	59
10 January 2013	4	27	11

Table 2
Overview showing the number of SMP field measurements, the verified danger level and the days since the last snowfall for the field campaigns.

Date	No. of SMP	Danger level	Days since snowfall
28 January 2011	125	low	2 days
3 March 2011	110	considerable	4 days
13 February 2012	119	moderate	19 days
9 March 2012	102	moderate	1 day
10 January 2013	157	moderate	3 days

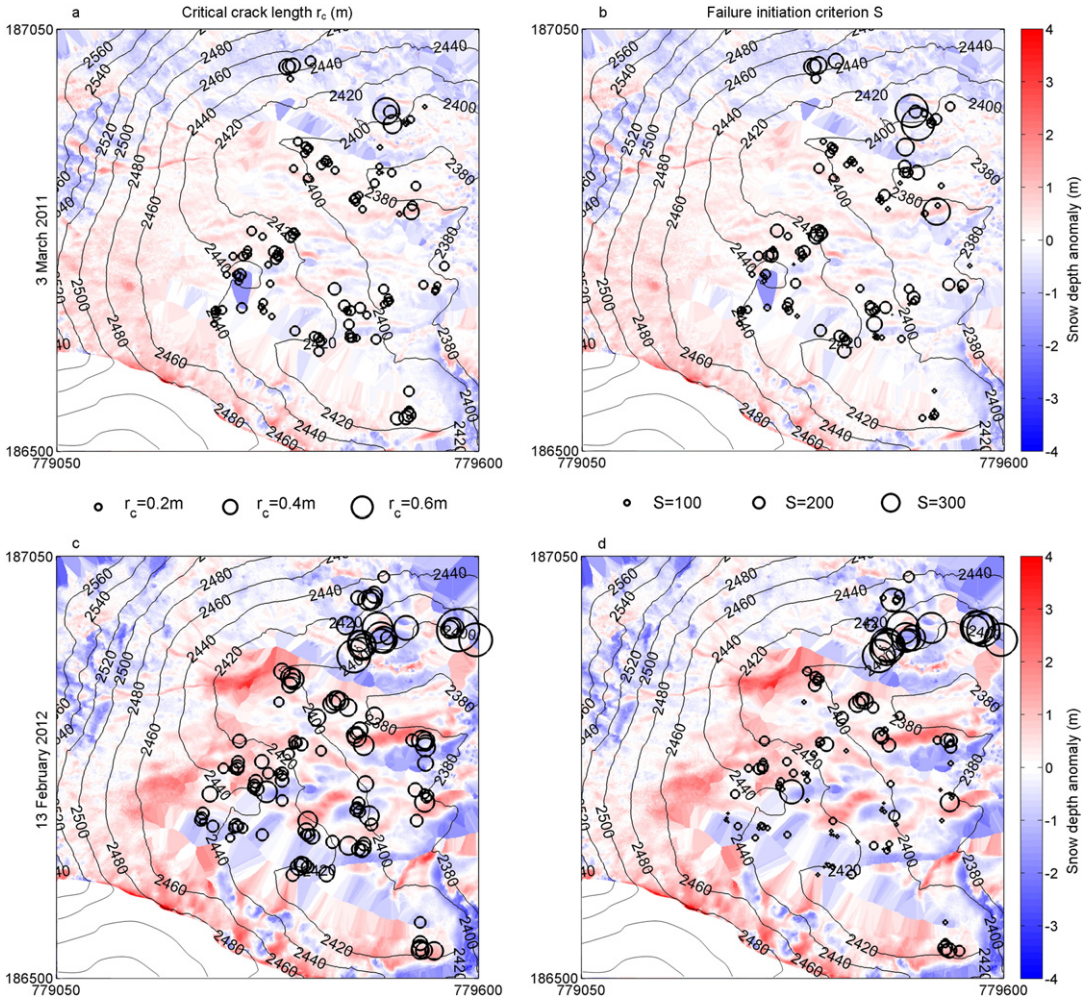

Fig. 4. Maps of snow depth anomaly, i.e. deviations from the daily mean snow depth for the Steintälli field site for 3 March 2011 (a, b) and 13 February 2012 (c, d). In addition, the modeled critical crack length r_c (a,c) and the failure initiation criterion S (b, d) are shown by circles; area of circles scales with magnitude of the values. Numbers indicate Swiss coordinates (in meters), i.e. an area of 550 m × 550 m is shown. Contour line spacing is 20 m of elevation.

was 'considerable'. On this day, we observed several whumpfs and also modeled short critical crack lengths (orange box in Fig. 5) confirming an increased propensity for crack propagation. A similar tendency was observed for the stability criterion S. However, the differences between the danger levels 'moderate' and 'considerable' were not as pronounced.

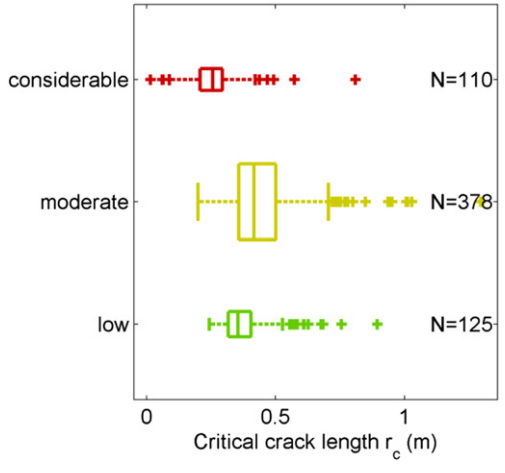

Fig. 5. Modeled critical crack length by verified avalanche danger level ($N = 613$). Width of boxes corresponds to the number of cases (see Table 2); whiskers extend to the most extreme data points not considered outliers (crosses) within 1.5 times the interquartile range above the 3rd and below the 1st quartile.

3.2. Simple drivers

We investigated the predictive power of slope aspect, snow depth and slope angle for the two modeled metrics of snow instability, and also related them to slab depth. In the following we present the results for the specific drivers, first by analyzing the field days all together, then by comparing the characteristics of the single field days.

3.2.1. Slope aspect

Considering all five field campaigns together, the aspect variable asp_{N-S} was not significantly related to our measures of instability. The aspect variable asp_{E-W}, however, showed statistically significant negative relations meaning that on slopes with aspects in the eastern half-space lower values of both, modeled critical crack length and stability criterion S were observed (Table 3). The polar plot in Fig. 6 shows the distribution of modeled critical crack length by aspect for the entire dataset. A slightly higher density of lower and intermediate values was found in the east-south-eastern (ESE) sector which together with the east-north-eastern (ENE) is contrasted with the NNE and SSE sectors and the NNW and the SSW sectors. The western sectors (WNW and WSW) had few cases and less influence on the trend of the aspect variable asp_{E-W}. The polar plot for the failure initiation criterion S looked similar.

Table 3
The *p*-values of the regression coefficients between potential drivers and the modeled critical crack length r_c as well as the stability criterion *S* shown for single field days and the entire dataset (all). Potential drivers: asp_{E-W} and asp_{N-S}, i.e. aspects in the eastern (northern) vs. aspects in the western (southern) half-space, snow depth and slope angle. Bold values indicate significance on a level of 5% and a regression coefficient standard error $\Delta(r) \leq 50\%$. Black colors denote a positive, blue colors a negative relationship.

Date	asp_{E-W}		asp_{N-S}		Snow depth		Slope angle	
	r_c	*S*	r_c	*S*	r_c	*S*	r_c	*S*
28 January 2011	0.18	**0.01**	0.08	0.47	0.06	**0.01**	**0.01**	0.85
3 March 2011	0.06	**0.02**	0.58	0.48	0.11	**0.03**	**0.01**	**0.01**
13 February 2012	**0.01**	**0.01**	**0.03**	**0.04**	0.64	0.21	0.07	0.78
9 March 2012	**0.01**	**0.01**	0.41	0.14	0.99	0.62	0.55	0.14
10 January 2013	0.88	0.82	**0.01**	**0.01**	0.72	**0.01**	0.06	**0.01**
All days	**0.01**	**0.01**	0.47	0.45	**0.01**	0.57	0.75	**0.01**

Considering the single days, both aspect variables were significant on 13 February 2012 (i.e. the *p*-values of the regression coefficients were $p \leq 0.05$) and hence aspect can be rated a dominant driver of both criteria, the failure initiation criterion and the critical crack length (columns 2–5 in Table 3). On the other days, however, at most one aspect variable was identified as a driver. On 13 February 2012 no new snow had been recorded since 18 days and meteorological processes such as radiation or snow drift had shaped the snowpack since. On the other field days upper slab layers were only 2–4 days old. On 9 March 2012, for instance, the snowfall had stopped the night before the field measurements were performed. On this day only the category asp_{E-W} was significant, other drivers were not significant. On the other hand, on 10 January 2013, the relation between the criteria of snowpack stability and asp_{N-S} was positive with lower stability on south-facing (than north-facing) slopes.

Fig. 4 contrasts the propensity for failure initiation and crack propagation of two situations. On 3 March 2011 (upper panels) asp_{N-S} was not a relevant driver, whereas on 13 February 2012 (lower panels) asp_{N-S} was a significant driver of both snow instability criteria. On 13 February 2012 values were lower in the central part than in the south-facing slopes in the northern part of the field site (lower panels). On 3 March 2011, however, this trend towards higher values of snow stability on south-facing slopes (upper panels) was not significant (Table 3).

3.2.2. Snow depth

Considering all five field campaigns together, snow depth was positively related with the modeled critical crack length (Table 3), i.e. with a deep snowpack a significantly lower propensity for crack propagation was modeled (Fig. 7). The correlation was fair ($r_p = 0.20$), but the linear trend was significant ($p < 0.01$). On the other hand, the relation between snow depth and the failure initiation criterion was not significant for the entire dataset.

In contrast to the findings for the entire dataset, snow depth was not related to the modeled critical crack length (Table 3) on any of the single days. Considering the other measure of instability, snow depth was positively related to the instability criterion *S* in two cases, namely on 28 January 2011 and 10 January 2013 (Table 3); this means the thicker the snowpack the harder failure initiation. On 3 March 2011, however, snow depth was negatively correlated with the instability criterion *S*.

In Fig. 4 snow depth anomalies from the daily mean are overlain with the modeled critical crack length and the failure initiation criterion. The distribution of snow depth was very similar on both days (and also on the other days; not shown). Consistent features were found in the northwestern corner of the maps where three finger-like features indicate large snow depths and in the central part where undulations of snow depth appear going from south to north. To some extent also the distributions of crack propagation and failure initiation propensity recurred. For both criteria the highest values were found on the south-facing slopes with a shallow snowpack. In the central part, however, differences of snow instability were not as clearly related to variations in snow depth. In summary, to some extent, large scale snow instability variations across our field site may be explained by snow depth variations, but features at a smaller scale, i.e. at the scale of tens of meters, do not seem to be related to patterns of snow depth.

3.2.3. Slope angle

If all field days were considered jointly, the slope angle was related to the failure initiation criterion, but not to the propensity of crack propagation. The sign of the regression coefficient (Table 3) indicated that on steeper slopes failures can be initiated more easily. Fig. 8 shows the distribution of the failure initiation criterion *S* for classes of slope angles. The median failure initiation criterion per class tended to decrease with increasing slope angle indicating easier failure initiation on steeper slopes ($r_p = -0.79, p = 0.03$). However, for the class with slope angles between 30° and 35°, including the steepest slopes we sample, the median value of *S* was slightly higher than for the preceding class; this increase is likely due to the fact that this class contains a small number of cases ($N = 40$) from south-facing slopes with rather high values of *S*.

Considering the single days, in three out of the four cases when slope angle was a driver of modeled snow instability, steeper slopes had higher values of critical crack length r_c or stability criterion *S* (Table 3). However, in our field site most steep slopes (>30°) are found on southerly aspects. Often we observed that slopes on southerly aspects were

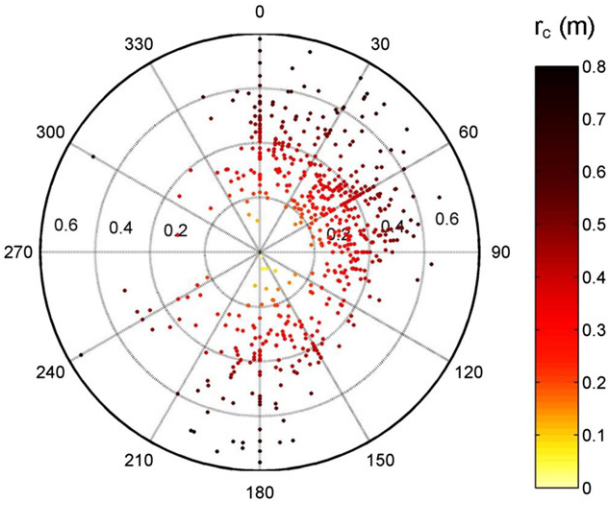

Fig. 6. Distribution of modeled critical crack length r_c by aspect (degrees from North) for all field measurements. Bright colors indicate short cut lengths ($N = 613$); eight outliers with $r_c > 0.8$ m are not shown.

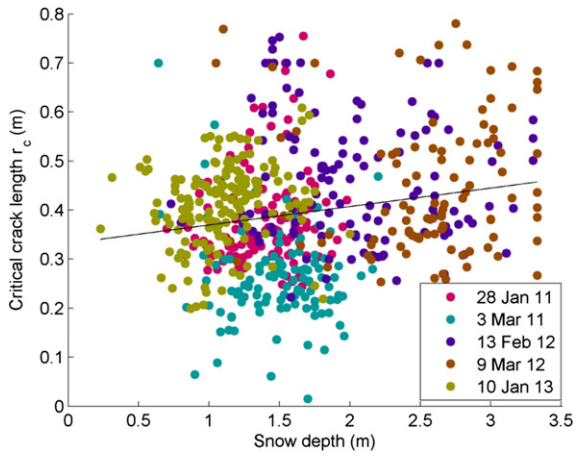

Fig. 7. Modeled critical crack length versus manually measured snow depth for all field days, indicated by different colors ($N = 613$); eight outliers with $r_c > 0.8$ m are not shown.

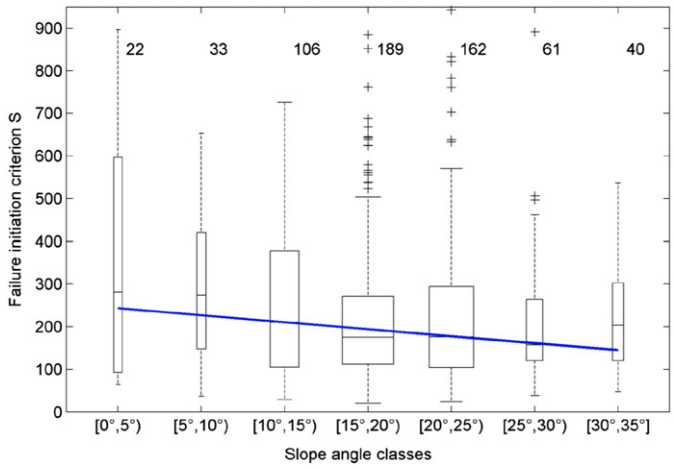

Fig. 8. Failure initiation criterion S for all field days versus classes of slope angle. Class '[0°, 5°)' covering $0° \le \alpha < 5°$, class '[5°, 10°)' covering $5° \le \alpha < 10°$, etc. The blue line indicates a robust regression for the bin medians weighted by their number of members. Width of boxes corresponds to the number of cases shown on the top ($N = 613$); five outliers with $S > 900$ are not shown.

less unstable, which may shift the proportion of unstable slopes among steep slopes towards more stable.

3.2.4. Slab depth

Performing a correlation analysis with slab depth led to very consistent, positive significant relations with the failure initiation criterion S (p-values $p < 0.05$ on all single days). Also, when considering the entire dataset slab depth was a significant positive driver with $p < 0.01$.

The crack propagation propensity was in three out of five cases significantly related with slab depth, but not considering the entire dataset ($p = 0.35$). In two cases (13 February 2012 and 9 March 2012) the relation was negative, i.e. below thicker slabs shorter critical crack lengths were modeled. In one case (3 March 2011), the relation was positive, in other words, below shallow slabs short critical crack lengths were modeled. There are plausible explanations for these seemingly contradictory findings. On one hand, thicker slabs release more energy and usually have shorter crack lengths given the same weak layer properties. On the other hand, weak layers below thicker slabs are stronger, i.e. have higher specific fracture energy resulting in longer critical crack lengths. However, based on our simple analysis we cannot tell which process, higher slab load or higher specific fracture energy, caused the relations we observed.

Slab depth was not correlated with snow depth ($r_p = -0.14$), i.e. snow depth should not be considered as an indicator of slab depth. Relationships of snow depth with the failure initiation criterion S existed on single days as shown above, but no clear relation was found for the entire dataset including all five field days. In cases when slab depth (i.e. weak layer depth) is known, for instance, when measuring or observing snow stratigraphy, more information on snow instability is already available and we would not rely on simple drivers.

4. Discussion

The layered structure of the snowpack suggests that temporary influences of external (e.g. wind) and internal (e.g. metamorphism) processes cause differences in layer properties (Schweizer et al., 2008b). The presented work aims at analyzing if simple drivers, which combine external and internal processes, are suitable for predicting differences in snow instability at the basin scale. With available objective measures of snow instability (Reuter et al., 2015), we were for the first time able to relate multiple objective measures of snow instability with terrain parameters and measurements of snow depth.

The failure initiation and the crack propagation propensity within the basin were mapped for two situations with danger level 'moderate' (13 February 2012) and 'considerable' (3 March 2011) (Fig. 4). Whereas the failure initiation criterion S was quite variable on 3 March 2011 and on 13 February 2012, the modeled critical crack length r_c showed less variable results on both days. On both days several locations existed where a failure could have been initiated, but on 13 February 2012 the crack propagation propensity was lower than on 3 March 2011 where especially in the central part of our field site modeled critical crack lengths were short. These qualitative results at the basin scale highlight the importance of the two separate processes, failure initiation and crack propagation with respect to snow instability. However, only a spatial analysis may allow assessing the influence of spatial variations on avalanche release.

Snow instability distributions within a region were investigated by Schweizer et al. (2003a) who evaluated manual observations and snow profiles from five field campaigns with varying avalanche conditions. They found distinct snow instability distributions for the three danger levels 'low', 'moderate' and 'considerable'. In our limited data set covering only 5 days we also obtained stability distributions (Fig. 5). The distributions were well representing the danger levels 'considerable' and 'moderate'. Still, our snow instability criteria did not reflect the lower propagation propensity on 1 day with danger level 'low', which may be due to the slab properties the algorithm currently still neglects, possibly the tensile strength of the slab. The results for our snow instability criteria showed the same behavior as in Schweizer et al. (2003a). Except for one situation on 28 January 2011 when due to a soft and low cohesion slab widespread avalanching was unlikely.

In our analysis, time spans between field campaigns and the last snowfall (deposition of the topmost slab layers) ranged from 1 to 19 days. On 13 February 2012 when the upper part of the slab was 19 days old, aspect was clearly a dominant driver. Both aspect variables were significant for both instability criteria. In the cases of more recently deposited slabs, differences in snow instability were not as much associated with slope aspect. Also right after storms, like on 9 March 2012, only one driver was found to be significant. Both results suggest that with aging of the slab layers the influence of the driver slope aspect on snow instability grew. Similar results were already presented by Birkeland (2001) who identified more drivers in his field campaigns after variable weather conditions than after sustained snow storms. Schweizer et al. (2008a) also observed less variation right after storms than after a subsequent fair weather period.

Snow instability patterns are supposed to be caused by terrain and weather conditions as atmospheric processes in combination with terrain set the boundary conditions for the evolution of the mountain snowpack (Schweizer et al., 2008b). The incoming radiation on a slope is a function of the incident angle. Hence, slope aspect plays a major role for the heat energy input into the snowpack and controls snow temperature and hence affects stability (Reuter and Schweizer, 2012). Also, snow deposition depends on slope aspect which is consequently anticipated to be a driver of snow density and hence stiffness. Differences in snow instability were in all cases related to aspect. This finding is in line with previous research, for instance with Schweizer et al. (2003b) who observed that often differences in snow instability were explained by aspect. Two variables were introduced explaining differences between easterly and westerly aspects which are likely caused by wind, and between northerly and southerly aspects which are likely caused by incoming shortwave radiation but also wind direction. We found that on east-facing slopes the propensity of failure initiation was higher in four out of five cases and of crack propagation in two out of five cases. With respect to north-south differences the aspect variable indicated significant trends in two cases, once with higher values on north-facing slopes than on south-facing ones, and once vice versa. Finding the reason for this discrepancy, would involve a more detailed analysis of all ingredients controlling our measures of snow instability

and their history, which is beyond the scope of this work. Already in a former study by Schweizer and Kronholm (2007) aspect was an important driver of weak layer presence. They explained surface hoar presence in one region with slope angle and the absolute deviation from north—similar to our aspect variable asp_{N-S}.

Also in our cases we found weak layers to be present over the entire basin, however, with varying strength and specific fracture energy. Internal processes such as sintering and metamorphism suggest that deeper snowpacks have weak layers which are stronger and not as prone to fracture under loading compared to shallower snowpacks (Jamieson et al., 2007). Snow depth was not related to the modeled critical crack length (Table 3) on any of the single days, but for the entire dataset snow depth was a significant driver. The failure initiation criterion was on three out of five field days driven by snow depth—with varying sign of correlation. Considering the entire dataset including all 5 days, a relation between snow depth and the failure initiation criterion was not found. Hence, on a single day, an association between snow depth and snow instability does not always exist, whereas on average, when we compare many different snow conditions we may observe a trend of increasing values of snowpack stability with increasing snow depth—controlled by the crack propagation propensity. Considering both, failure initiation and crack propagation as required ingredients of snow instability our findings agree with frequently reported significant positive correlations between snow depth and snow stability for different observation times and field sites with varying snowpack conditions at the regional scale (Schweizer et al., 2003b; Zeidler and Jamieson, 2004). An anticipated relation between the failure initiation criterion and snow depth on average, i.e. for the entire dataset, was not confirmed. Our measurements of snow depth were not even correlated with slab depth, which is closely tied to failure initiation.

We found recurring patterns of snow depth in accordance with previous studies (Grünewald et al., 2010). Also, some patterns of the crack propagation and failure initiation propensity recurred. Values were highest on south-facing slopes with a shallow snowpack in the northern part of our field site, whereas differences of snow instability were not as clearly related to variations of snow depth within the central part of our basin. It seems that snow depth variations can explain patterns of snow instability on a larger scale, such as across our field site, but are not necessarily indicative of small scale variations of snow instability at the scale of tens of meters.

We excluded slab depth from the MLR analysis, as it is no simple driver, i.e. there is no widespread data available on the depth of the weak layer. Automated, repeated LIDAR measurements could provide this piece of information, provided the exact burial time of the relevant weak layer is known and snow settlement is negligible.

Slope angle affects the incident solar radiation and hence partly controls snow temperature. Snow instability also directly depends on slope angle, as with slope incline the stress state due to loading shifts towards higher shear and lower normal stresses. On single days, we observed three times positive and once negative relations with our measures of snow instability in the four cases when slope angle was a driver. This finding is somewhat counterintuitive. If we consider, for example, the definition of the skier stability index where the shear stress increases with increasing slope angle, lower values of the skier stability index are expected on steeper slopes. However, the distribution of steep slopes (>30°) within our field site is imbalanced towards considerably more cases on south-facing slopes. In other words, the stability might have been simply less critical on the south-facing slopes which at the same time are the steepest ones we usually sample. Thus, results for single days are questionable. The entire dataset representing many different snowpack conditions, however, showed that the slope angle played a significant role in controlling the failure initiation propensity. Decreasing values of the failure initiation criterion S, i.e. failure is more likely, were associated with increasing slope angle. In the past, studies investigating the role of the slope angle as a potential driver of snow instability found contradicting results. Previous studies presented field data on the crack propagation propensity (Gauthier and Jamieson, 2008a; Heierli et al., 2011), on the propensity of failure initiation based on ECT scores on slopes (e.g. Simenhois et al., 2012) and on snow instability in general (Schweizer et al., 2003a) and did not find a significant relation with slope angle. Jamieson (1999) and Campbell and Jamieson (2007), however, found a correlation of decreasing compression and Rutschblock test scores with increasing slope angle, respectively. In this study, however, snow instability was modeled with a two-step approach considering failure initiation and crack propagation, two important requirements for slab avalanche release. Our results suggest a slight increase of the failure initiation propensity with slope angle, which is the first step in the chain of events preceding avalanche release.

The data on simple drivers we presented were determined from manual field observations with typical observation uncertainties of about 5° for aspects, 1 cm for snow depth and 3° for slope angles. Snow instability data were derived from post-processed snow micro-penetrometer signals representing several sources of uncertainty. The uncertainty can be assessed in comparisons with experimental data and yields about 2 cm for modeled critical crack lengths (RMSE) and about one Rutschblock score for the modeled failure initiation criterion (Reuter et al., 2015); this roughly corresponds to an uncertainty $\Delta(S) \approx 40$. The snow depth derived from TLS measurements has an accuracy of about 10 cm (Grünewald et al., 2010).

5. Conclusions

We presented an application of a new method to derive point snow instability from SMP measurements allowing observer-independent measurements of snow instability. By performing multiple spatially distributed snow micro-penetrometer measurements in a small alpine basin we obtained a unique dataset covering five different avalanche situations. Maps from two different snow instability situations provided a qualitative picture of the spatial distribution of snow instability with respect to the propensity of failure initiation and crack propagation. Our measures of snow instability were able to reproduce snow instability distributions characteristic of the avalanche danger level as observed in previous studies.

Following our hypothesis that simple drivers may explain differences in snow instability to a significant extent, we related our objective measurements of snow instability to simple drivers, rather than process drivers: slope aspect, snow depth and slope angle. The most prominent driver was slope aspect. We observed that the older the slab was the more differences of snow instability were reflected in the driver aspect. In our field site significant differences of snow instability existed between east-facing and west-facing slopes. On single field days a stepwise MLR analysis showed different relationships, positive and negative, between drivers and our measures of snow instability depending on the situation. Applying the analysis on the entire dataset which contains many different snow conditions revealed that snow depth was a driver of the crack propagation propensity and slope angle was a driver of the failure initiation propensity. Briefly, on average, thicker snowpacks tended to produce longer critical crack lengths and on steeper slopes failure initiation was easier. Our results compared well with previous studies identifying aspect and snow depth as important drivers of snow instability at the slope as well as at the regional scale. Furthermore, slab depth was very clearly positively related with the failure initiation criterion S confirming that a failure is more easily initiated below a shallow slab.

Also, this study sheds new light on the role of the slope angle in view of snow instability which was often controversially discussed. Our results suggest that slope angle mainly controls the propensity of failure initiation and thus influences snow instability since both criteria need to be fulfilled for avalanche formation (Reuter et al., 2015). In our field data set the modeled critical crack length, however, never significantly decreased with increasing slope angle. This trend was anticipated

from the knock-down function presented by Gaume et al. (2014), but was not verified in the field, yet.

Recurring patterns of snow depth could only to some extent explain differences in snow instability. To better resolve small scale patterns of snow instability and explore relations with external drivers a geostatistical analysis of the presented dataset will be required.

To sum up, simple drivers exist and may help to enhance our predictions of snow instability, but we should bear in mind the influences to avoid over-interpreting. Certainly, micro-meteorological and snow cover modeling have the potential to account for external and internal drivers separately and will be a logical next step. Nonetheless, due to their good availability and their ties with the processes influencing snow instability exploring the role of simple drivers seems worthwhile. The processes shaping the mountain snowpack and hence controlling snow instability are complex and may not be reflected in a set of drivers. With this in mind the results may be valuable for snow instability estimations, where direct information of snow instability is lacking between point observations, e.g. when applying forecasting models in data sparse areas or verifying snow instability distributions from measured data in large areas.

Acknowledgements

We are grateful for the comments by two anonymous reviewers that helped to improve the manuscript. We would like to thank all colleagues involved in the field campaigns, in particular Thomas Grünewald, Anna Haberkorn, Christoph Mitterer, Lino Schmid, Stephan Simioni and Walter Steinkogler. B.R. has been supported by a grant of the Swiss National Science Foundation (200021_144392).

References

Birkeland, K.W., 2001. Spatial patterns of snow stability throughout a small mountain range. J. Glaciol. 47 (157), 176–186.
Birkeland, K.W., Hansen, H.J., Brown, R.L., 1995. The spatial variability of snow resistance on potential avalanche slopes. J. Glaciol. 41 (137), 183–189.
Blöschl, G., Sivapalan, M., 1995. Scale issues in hydrological modelling—a review. Hydrol. Process. 9, 251–290.
Borish, M., Birkeland, K.W., Custer, S., Challender, S., Hendrikx, J., 2012. Surface hoar distribution at the scale of a helicopter skiing operation. Proceedings ISSW 2012, International Snow Science Workshop, Anchorage AK, U.S.A., 16-21 September 2012, pp. 1040–1046.
Campbell, C., Jamieson, J.B., 2007. Spatial variability of slab stability and fracture characteristics within avalanche start zones. Cold Reg. Sci. Technol. 47 (1-2), 134–147.
Dadic, R., Mott, R., Lehning, M., Burlando, P., 2010. Wind influence on snow depth distribution and accumulation over glaciers. J. Geophys. Res. 115, F01012. http://dx.doi.org/10.1029/2009JF001261.
Draper, N.R., Smith, H., 1998. Applied Regression Analysis. Wiley Series in Probability and Statistics. John Wiley & Sons.
Feick, S., Kronholm, K., Schweizer, J., 2007. Field observations on spatial variability of surface hoar at the basin scale. J. Geophys. Res. 112 (F2), F02002. http://dx.doi.org/10.1029/2006JF000587.
Gaume, J., Schweizer, J., van Herwijnen, A., Chambon, G., Reuter, B., Eckert, N., Naaim, M., 2014. Evaluation of slope stability with respect to snowpack spatial variability. J. Geophys. Res. 119 (9), 1783–1799.
Gauthier, D., Jamieson, B., 2008a. Evaluation of a prototype field test for fracture and failure propagation propensity in weak snowpack layers. Cold Reg. Sci. Technol. 51 (2-3), 87–97.
Gauthier, D., Jamieson, B., 2008b. Fracture propagation propensity in relation to snow slab avalanche release: validating the propagation saw test. Geophys. Res. Lett. 35 (13), L13501.
Grünewald, T., Schirmer, M., Mott, R., Lehning, M., 2010. Spatial and temporal variability of snow depth and ablation rates in a small mountain catchment. Cryosphere 4 (2), 215–225.
Grünewald, T., Stötter, J., Pomeroy, J.W., Dadic, R., Banos, I.M., Marturia, J., Spross, M., Hopkinson, C., Burlando, P., Lehning, M., 2013. Statistical modelling of the snow depth distribution in open alpine terrain. Hydrol. Earth Syst. Sci. 17 (8), 3005–3021.
Habermann, M., Schweizer, J., Jamieson, J.B., 2008. Influence of snowpack layering on human-triggered snow slab avalanche release. Cold Reg. Sci. Technol. 54 (3), 176–182.
Haladuick, S., Schirmer, M., Jamieson, B., 2014. What do field observations tell us about avalanche danger? In: Haegeli, P. (Ed.), Proceedings ISSW 2014. International Snow Science Workshop, Banff, Alberta, Canada, 29 September–3 October 2014, pp. 63–66
Heierli, J., Birkeland, K.W., Simenhois, R., Gumbsch, P., 2011. Anticrack model for skier triggering of slab avalanches. Cold Reg. Sci. Technol. 65 (3), 372–381.
Helbig, N., van Herwijnen, A., 2012. Modeling the spatial distribution of surface hoar in complex topography. Cold Reg. Sci. Technol. 82, 68–74.
Helbig, N., Löwe, H., Mayer, B., Lehning, M., 2010. Explicit validation of a surface shortwave radiation balance model over snow-covered complex terrain. J. Geophys. Res. 115, D18113. http://dx.doi.org/10.1029/2010JD013970.
Horton, S., Schirmer, M., Jamieson, B., 2015. Meteorological, elevation, and slope effects on surface hoar formation. Cryosphere Discuss. 9, 1857–1885.
Jamieson, J.B., 1999. The compression test—after 25 years. Avalanche Rev. 18 (1), 10–12.
Jamieson, J.B., Johnston, C.D., 1997. The compression test for snow stability. Proceedings ISSW 1996, International Snow Science Workshop, Banff, Alberta, Canada, 6-10 October 1996. Canadian Avalanche Association, Revelstoke BC, Canada, pp. 118–125.
Jamieson, J.B., Johnston, C.D., 1998. Refinements to the stability index for skier-triggered dry slab avalanches. Ann. Glaciol. 26, 296–302.
Jamieson, B., Zeidler, A., Brown, C., 2007. Explanation and limitations of study plot stability indices for forecasting dry snow slab avalanches in surrounding terrain. Cold Reg. Sci. Technol. 50 (1-3), 23–34.
Jamieson, B., Haegeli, P., Schweizer, J., 2009. Field observations for estimating the local avalanche danger in the Columbia Mountains of Canada. Cold Reg. Sci. Technol. 58 (1-2), 84–91.
Johnson, J.B., Schneebeli, M., 1999. Characterizing the microstructural and micromechanical properties of snow. Cold Reg. Sci. Technol. 30 (1-3), 91–100.
Landry, C., Birkeland, K., Hansen, K., Borkowski, J., Brown, R., Aspinall, R., 2004. Variations in snow strength and stability on uniform slopes. Cold Reg. Sci. Technol. 39 (2-3), 205–218.
Löwe, H., van Herwijnen, A., 2012. A Poisson shot noise model for micro-penetration of snow. Cold Reg. Sci. Technol. 70, 62–70.
Lutz, E.R., Birkeland, K.W., 2011. Spatial patterns of surface hoar properties and incoming radiation on an inclined forest opening. J. Glaciol. 57 (202), 355–366.
Marshall, H.-P., Johnson, J.B., 2009. Accurate inversion of high-resolution snow penetrometer signals for microstructural and micromechanical properties. J. Geophys. Res. 114 (F4), F04016. http://dx.doi.org/10.1029/2009jf001269.
Mott, R., Lehning, M., 2010. Meteorological modelling of very high resolution wind fields and snow deposition for mountains. J. Hydrometeorol. 11 (4), 934–949.
Prokop, A., 2008. Assessing the applicability of terrestrial laser scanning for spatial snow depth measurements. Cold Reg. Sci. Technol. 54 (3), 155–163.
Prokop, A., Schirmer, M., Rub, M., Lehning, M., Stocker, M., 2008. A comparison of measurement methods: terrestrial laser scanning, tachymetry and snow probing, for the determination of the spatial snow depth distribution on slopes. Ann. Glaciol. 49, 210–216.
Proksch, M., Löwe, H., Schneebeli, M., 2015. Density, specific surface area and correlation length of snow measured by high-resolution penetrometry. J. Geophys. Res. 120 (2), 346–362.
Reuter, B., Schweizer, J., 2012. The effect of surface warming on slab stiffness and the fracture behavior of snow. Cold Reg. Sci. Technol. 83–84, 30–36.
Reuter, B., Proksch, M., Loewe, H., van Herwijnen, A., Schweizer, J., 2013. On how to measure snow mechanical properties relevant to slab avalanche release. In: Naaim-Bouvet, F., Durand, Y., Lambert, R. (Eds.), Proceedings ISSW 2013. International Snow Science Workshop, Grenoble, France, 7-11 October 2013. ANENA, IRSTEA, Météo-France, Grenoble, France, pp. 7–11.
Reuter, B., Schweizer, J., van Herwijnen, A., 2015. A process-based approach to estimate snow instability. Cryosphere 9, 837–847.
Schirmer, M., Wirz, V., Clifton, A., Lehning, M., 2011. Persistence in intra-annual snow depth distribution: 1. Measurements and topographic control. Water Resour. Res. 47, W09516.
Schneebeli, M., Johnson, J.B., 1998. A constant-speed penetrometer for high-resolution snow stratigraphy. Ann. Glaciol. 26, 107–111.
Schweizer, J., Jamieson, J.B., 2007. A threshold sum approach to stability evaluation of manual snow profiles. Cold Reg. Sci. Technol. 47 (1-2), 50–59.
Schweizer, J., Jamieson, J.B., 2010. Snowpack tests for assessing snow-slope instability. Ann. Glaciol. 51 (54), 187–194.
Schweizer, J., Kronholm, K., 2007. Snow cover spatial variability at multiple scales: characteristics of a layer of buried surface hoar. Cold Reg. Sci. Technol. 47 (3), 207–223.
Schweizer, J., Reuter, B., 2015. A new index combining weak layer and slab properties for snow instability prediction. Nat. Hazards Earth Syst. Sci. 15, 109–118.
Schweizer, J., Jamieson, J.B., Schneebeli, M., 2003a. Snow avalanche formation. Rev. Geophys. 41 (4), 1016. http://dx.doi.org/10.1029/2002RG000123.
Schweizer, J., Kronholm, K., Wiesinger, T., 2003b. Verification of regional snowpack stability and avalanche danger. Cold Reg. Sci. Technol. 37 (3), 277–288.
Schweizer, J., Heilig, A., Bellaire, S., Fierz, C., 2008a. Variations in snow surface properties at the snowpack depth, the slope and the basin scale. J. Glaciol. 54 (188), 846–856.
Schweizer, J., Kronholm, K., Jamieson, J.B., Birkeland, K.W., 2008b. Review of spatial variability of snowpack properties and its importance for avalanche formation. Cold Reg. Sci. Technol. 51, 253–272.
Schweizer, J., van Herwijnen, A., Reuter, B., 2011. Measurements of weak layer fracture energy. Cold Reg. Sci. Technol. 69 (2-3), 139–144.
Simenhois, R., Birkeland, K.W., 2009. The Extended Column Test: test effectiveness, spatial variability, and comparison with the Propagation Saw Test. Cold Reg. Sci. Technol. 59 (2-3), 210–216.
Simenhois, R., Birkeland, K.W., van Herwijnen, A., 2012. Measurements of ECT scores and crack-face friction in non-persistent weak layers: what are the implications for practitioners? Proceedings ISSW 2012. International Snow Science Workshop ISSW 2012, Anchorage AK, U.S.A., 16-21 September 2012, pp. 104–110
Sturm, M., Benson, C.S., 2004. Scales of spatial heterogeneity for perennial and seasonal snow layers. Ann. Glaciol. 38, 253–260.

van Herwijnen, A., Heierli, J., 2010. A field method for measuring slab stiffness and weak layer fracture energy. Proceedings ISSW 2010, International Snow Science Workshop, Lake Tahoe CA, U.S.A., 17-22 October 2010, pp. 232–237.
van Herwijnen, A., Jamieson, J.B., 2007. Snowpack properties associated with fracture initiation and propagation resulting in skier-triggered dry snow slab avalanches. Cold Reg. Sci. Technol. 50 (1-3), 13–22.
Veitinger, J., Sovilla, B., Purves, R.S., 2014. Influence of snow depth distribution on surface roughness in alpine terrain: a multi-scale approach. Cryosphere 8 (2), 547–569.
Winstral, A., Elder, K., Davis, R.E., 2002. Spatial snow modeling of wind-redistributred snow using terrain based parameters. J. Hydrometeorol. 3 (5), 524–538.
Winstral, A., Marks, D., Gurney, R., 2009. An efficient method for distributing wind speeds over heterogeneous terrain. Hydrol. Process. 23 (17), 2526–2535.
Zeidler, A., Jamieson, J.B., 2004. A nearest-neighbour model for forecasting skier-triggered dry-slab avalanches on persistent weak layers in the Columbia Mountains, Canada. Ann. Glaciol. 38, 166–172.